

## SUPPORTING INFORMATION

# Effect of environment medium and the *in situ* formation of precursor on the composition-shape of iron oxide nanoparticles synthesized by thermal decomposition method

Walid Baaziz,<sup>1,\*</sup> Benoit P. Pichon,<sup>1</sup> Jean-Marc Grenèche,<sup>2</sup> Sylvie Begin-Colin<sup>1,\*</sup>

<sup>1</sup> Institut de Physique et Chimie des Matériaux de Strasbourg (IPCMS), UMR 7504 du CNRS, Université de Strasbourg, 23 rue du Loess, 67037 Strasbourg Cedex 02, France

<sup>2</sup> Institut des Molécules et Matériaux du Mans IMMM UMR CNRS 6283, Université du Maine, Avenue Olivier Messiaen, 72085 Le Mans Cedex 9, France

**Figure S1:** TGA curves of iron stearate (black line) and iron oleate (red line) carried out under air with a heating rate of 5°C/min.

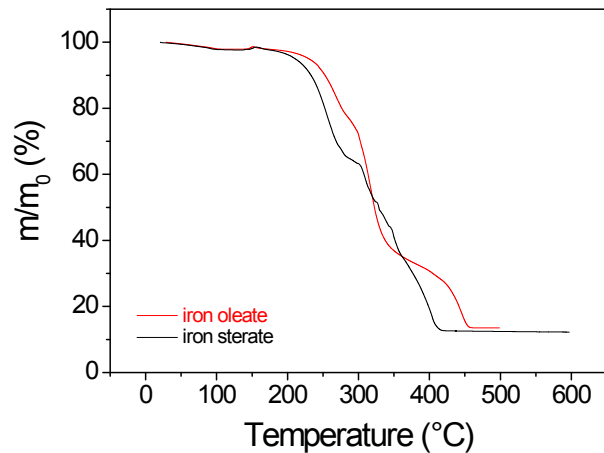


**Table S1 :**  $1/d_{(hkl)}$  measured from the electronic diffraction pattern in Fig. 2e, corresponding  $d_{(hkl)}$ ,  $(hkl)$  plans and theoretic  $d_{(hkl)}$  of magnetite (JCPDS card n° 00-019-0629).

$1/d_{(hkl)}$ measured ( $\text{\AA}^{-1}$ ) ¹)	$d_{(hkl)}$ measured ( $\text{\AA}$ )	$(hkl)$	$d_{(hkl)}$ of $\text{Fe}_3\text{O}_4$ ( $\text{\AA}$ )
0.322	3.11	(220)	2.965
0.376	2.66	(311)	2.529
0.450	2.22	(400)	2.097
0.585	1.71	(422)	1.924
0.633	1.58	(511)	1.614
0.734	1.36	(440)	1.483
0.774	1.29	(533)	1.279
0.856	1.17	(444)	1.211
0.889	1.12	(731)	1.092

**Table S2 :**  $1/d_{(hkl)}$  measured from the electronic diffraction pattern in Fig. 2f, corresponding  $d_{(hkl)}$ ,  $(hkl)$  plans and theoric  $d_{(hkl)}$  of magnetite (JCPDS card n° 00-019-0629) and wustite (JCPDS card n° 00-006-0615).

		Magnetite $\text{Fe}_3\text{O}_4$		Wüstite $\text{FeO}$	
$1/d_{(hkl)}$ measured ( $\text{\AA}^{-1}$ )	$d_{(hkl)}$ measured ( $\text{\AA}$ )	$(hkl)$	Theoretical $d_{(hkl)}$ ( $\text{\AA}$ )	$(hkl)$	Theoretical $d_{(hkl)}$ ( $\text{\AA}$ )
0.67	1.49	(440)	1.483	(220)	1.523
0.63	1.58	(511)	1.614		
0.474	2.11	(400)	2.097	(200)	2.153
0.4	2.5	(311)	2.529	(111)	2.49
0.341	2.93	(220)	2.965		

**Figure S2:** DRX pattern of nanoparticles NSC16, refined with considering spinel and wustite components (on top) and considering just one spinel phase (down).

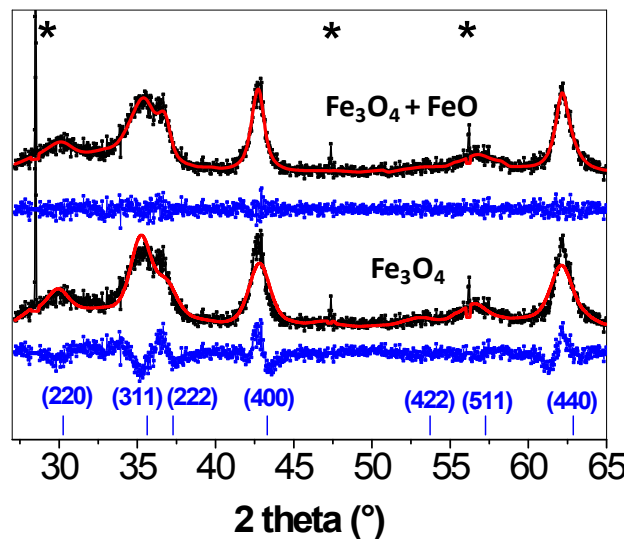


**Figure S3:**  $^{57}\text{Fe}$  Mössbauer spectra measured at 300 K of NSH11 (A), at 77 K of NSH11 and NSH16 (B,C) and at 11 K under a magnetic field of 8 T of NSH11 (D).

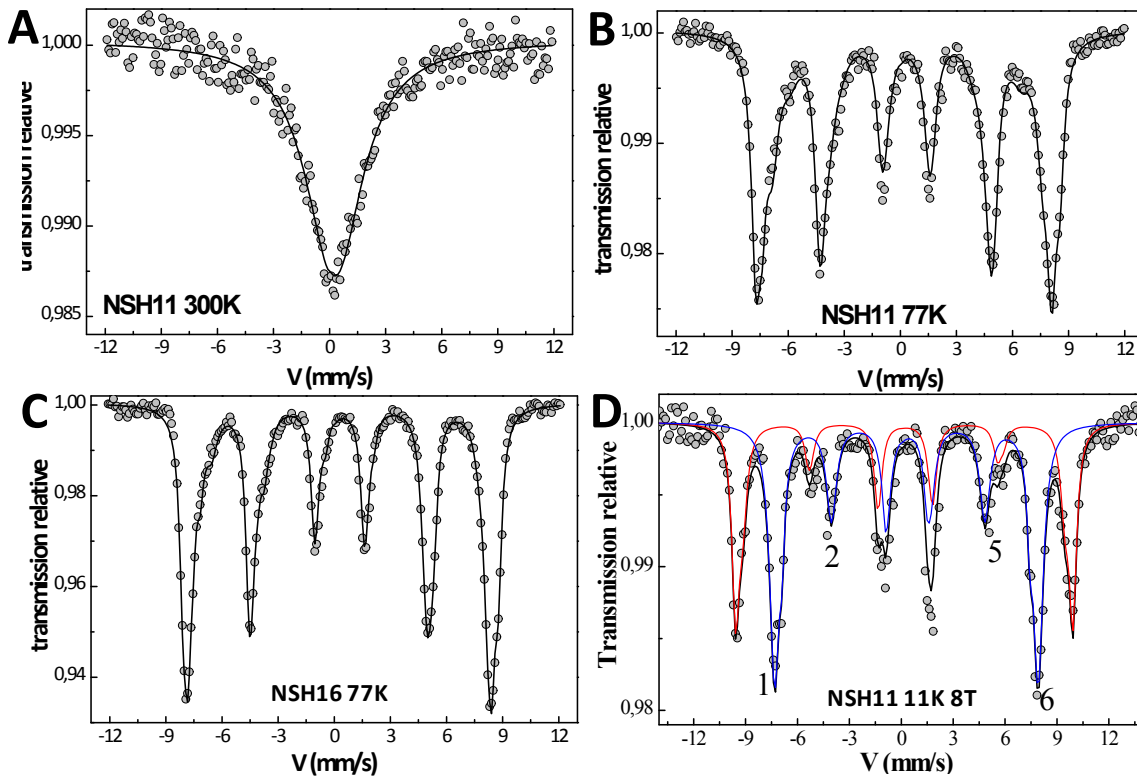


**Figure S4:** Magnetization curves as function of an applied field at 5 K after cooling without (ZFC) and with (FC) an applied field of 4 T of nanoparticles NSH11 and NSC11.

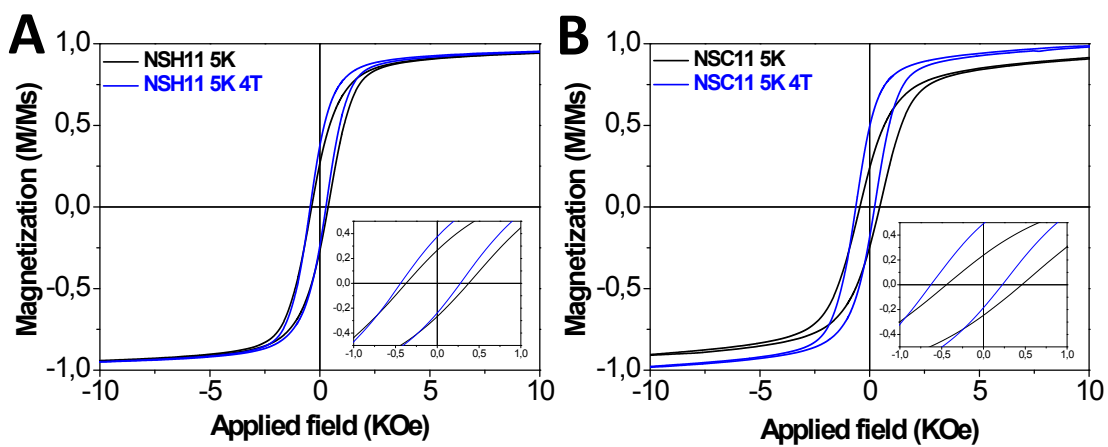


**Figure S5:** Iron oxide NPs synthesized from the thermal decomposition of iron stearate in similar conditions described in the paragraph 2.2.1.

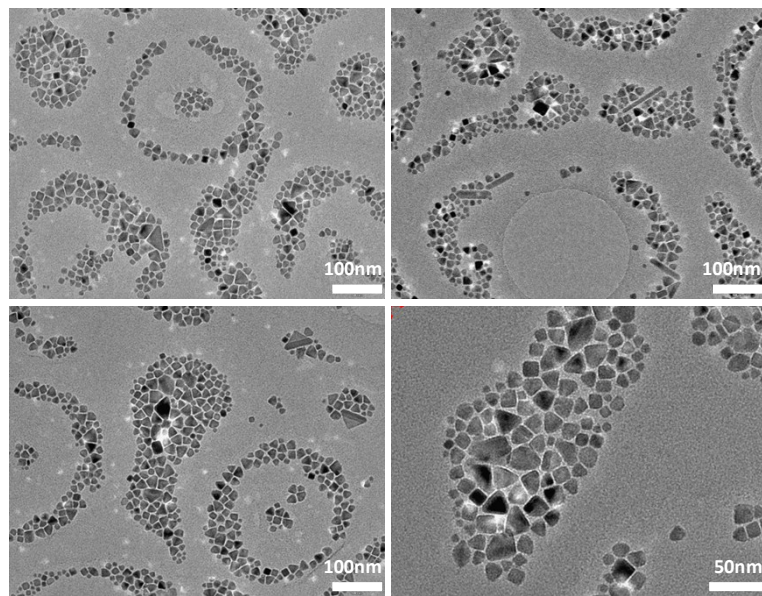


**Figure S6:**  $^{57}\text{Fe}$  Mössbauer spectra of nanoparticles NCH14 measured at 300 K (A) and 77 K (B).

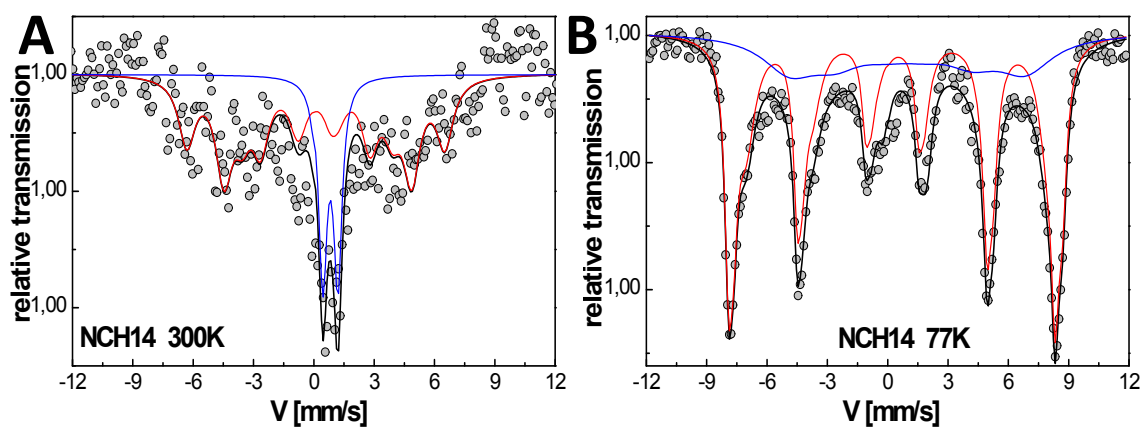


**Figure S7:** Magnetization curves as function of an applied field at 5 K after cooling without (ZFC) and with (FC) an applied field of 4 T of nanoparticles NCC16.

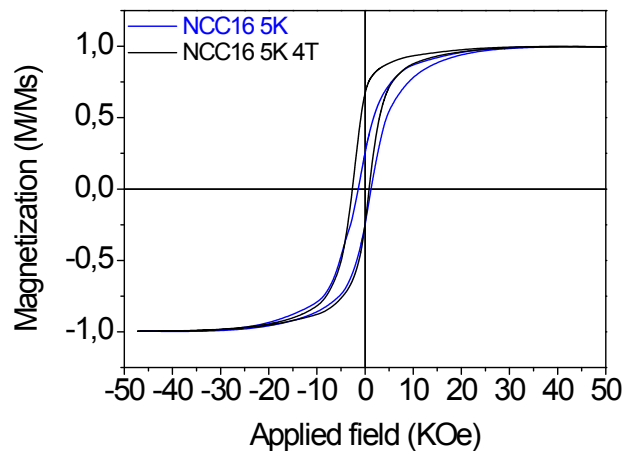


**Table S3:** Values of the exchange field ( $H_E$ ) of nanoparticles NCH14 as a function of the temperature measured from the magnetization curves present in Fig.11.

Temperature (K)	Exchange Field $H_E$ (Oe)
5	41,2
10	38,55
20	28,45
30	15,25
40	10,55
50	8,6